

# Proton Conduction in Thickness-Controlled Ultrathin Polycation/Nafion Multilayers Prepared via Layer-by-Layer Assembly

Yusuke Daiko,<sup>†</sup> Kiyofumi Katagiri,<sup>‡</sup> and Atsunori Matsuda<sup>\*,§</sup>

Department of Materials and Chemistry, University of Hyogo, Shosha, Himeji, Hyogo 671-2101, Japan,  
Department of Applied Chemistry, Graduate School of Engineering, Nagoya University, Nagoya,  
Aichi 464-8603, Japan, and Department of Materials Science, Toyohashi University of Technology,  
Tempaku, Toyohashi, Aichi 441-8580, Japan

Received March 17, 2008. Revised Manuscript Received September 1, 2008

Ultrathin layers of positively charged poly(allylamine hydrochloride) (PAH) and a negatively charged high-proton conductor of Nafion were alternately deposited via layer-by-layer assembly. The incremental film growth of PAH and Nafion multilayers was monitored using a quartz crystal microbalance (QCM). The results obtained using the QCM revealed that each PAH/Nafion multilayer was deposited regularly and homogeneously. The  $\zeta$ -potential and thickness of the Nafion layer, which are related to the concentration of free  $-\text{SO}_3^-$  groups, were changed significantly by varying the pH of the PAH solution used. The thickness of one Nafion layer was controlled in the range from approximately 4 to 15 nm. The surface charge density of the PAH/Nafion multilayer was estimated using a Poisson–Boltzmann equation. A linear relationship between the proton conductivity and surface charge density of the outmost Nafion layer was observed. Furthermore, the proton mobility of the PAH/Nafion multilayer ( $15.2 \text{ cm}^2/(\text{V s})$ ) was about sevenfold higher than that of a bulk Nafion membrane ( $2.0 \text{ cm}^2/(\text{V s})$ ).

## Introduction

Solid state ionic conductors have attracted considerable attention and have been widely studied for applications as capacitors, sensors, and fuel cells. One crucial aspect for practical applications of solid electrolytes is the improvement in their ionic conductivity. In 1973, Liang first reported that lithium ion conductivity was increased by more than 1 order of magnitude by dispersing an insulator of small  $\text{Al}_2\text{O}_3$  particles.<sup>1</sup> Since then, there has been growing interest in the “heterointerface” of composite electrolytes as a fast-ionic-transfer field. The dispersion of insoluble, dielectric oxide particles in various solid electrolytes, such as  $\text{LiI}-\text{Al}_2\text{O}_3$ ,<sup>1</sup>  $\text{CuCl}_2-\text{Al}_2\text{O}_3$ ,<sup>2</sup>  $\text{AgI}-\text{Al}_2\text{O}_3$ ,<sup>3–5</sup>  $\text{PEO}/\text{LiClO}_4-\text{Al}_2\text{O}_3$ ,<sup>6</sup>  $\text{PEO}/\text{LiClO}_4-\text{BaTiO}_3$ ,<sup>7</sup> and  $\text{AgI}-\text{TiO}_2$ ,<sup>8</sup> was found to enhance the ionic conductivity of the electrolytes.

On the other hand, it has been demonstrated that nanometer-scale multilayers of solid electrolytes can realize artificial heterointerfaces, where large enhancements of ionic

conductivities including those of  $\text{Li}^+$ ,<sup>9–11</sup>  $\text{F}^-$ ,<sup>12,13</sup>  $\text{O}^{2-}$ ,<sup>14,15</sup>  $\text{Ag}^+$ ,<sup>16</sup> and  $\text{H}^+$ <sup>17</sup> have also been reported thus far. Another important finding is that Maekawa et al. reported that a  $\text{LiI}$  electrolyte infiltrating nanosized pores of mesoporous  $\text{Al}_2\text{O}_3$  showed a much higher  $\text{Li}^+$  ion conductivity than the bulk  $\text{LiI}$ .<sup>18</sup>

One explanation for the enhancement of ionic conductivity is that the concentration of ionic defects increases in the space-charge region near the heterointerfaces.<sup>2</sup> The space-charge region has been characterized by the Debye screening length  $\lambda_D$ . Since the  $\lambda_D$  in a solid state ionic conductor ranges from a few to several tens of nanometers, the preparation and ionic conduction mechanism of a nanostructured solid electrolyte have been extensively studied. Maier<sup>19–22</sup> and

\* Corresponding author. Fax: +81 532 48-5833. E-mail: matsuda@tutms.tut.ac.jp.

<sup>†</sup> University of Hyogo.

<sup>‡</sup> Nagoya University.

<sup>§</sup> Toyohashi University of Technology.

- (1) Liang, C. C. *J. Electrochem. Soc.* **1973**, *120*, 1289–1292.
- (2) Jow, T.; Wagner, J. B. *J. Electrochem. Soc.* **1979**, *126*, 1963–1972.
- (3) Shai, K.; Wagner, J. B. *J. Electrochem. Soc.* **1980**, *128*, 6–13.
- (4) Schmidt, J. A.; Bazán, J. C.; Vico, L. *Solid State Ionics* **1988**, *27*, 1–4.
- (5) Tadanaga, K.; Imai, K.; Tatsumisago, M.; Minami, T. *J. Electrochem. Soc.* **2000**, *147*, 4061–4064.
- (6) Croce, F.; Appetecchi, G. B.; Persi, L.; Scrosati, B. *Nature* **1998**, *394*, 456–458.
- (7) Sun, H.-Y.; Sohn, H.-J.; Yamamoto, O.; Takeda, Y.; Imanishi, N. *J. Electrochem. Soc.* **1999**, *146*, 1672–1676.
- (8) Furusawa, S.; Miyaoka, S.; Ishibashi, Y. *J. Phys. Soc. Jpn.* **1991**, *60*, 1666–1671.

- (9) Schreck, E.; Lauser, K.; Dransfeld, H. *Z. Phys. B. Condens. Matter* **1986**, *62*, 331–334.
- (10) Lubben, D.; Modine, F. A. *J. Appl. Phys.* **1996**, *80*, 5150–5157.
- (11) Furusawa, S.; Shimizu, S.; Sekine, K.; Tabuchi, H. *Solid State Ionics* **2004**, *167*, 325–329.
- (12) Modine, F. A.; Lubben, D.; Bates, J. B. *J. Appl. Phys.* **1993**, *74*, 2658–2664.
- (13) Sata, N.; Eberman, K.; Eberl, K.; Maier, J. *Nature* **2000**, *408*, 946–949.
- (14) Azad, S.; Marina, O. A.; Wang, C. M.; Saraf, L.; Shutthanandan, V.; McCready, D. E.; El-Azab, A.; Jaffe, J. E.; Engelhard, M. H.; Peden, C. H. F.; Thevuthasan, S. *Appl. Phys. Lett.* **2005**, *86*, 131906.
- (15) Peters, A.; Korte, C.; Hesse, D.; Zakherov, N.; Janek, J. *Solid State Ionics* **2007**, *178*, 67–76.
- (16) Muhlherr, S.; Lauser, K.; Schreck, E.; Dransfeld, K. *Solid State Ionics* **1988**, *28–30*, 1495–1505.
- (17) Kuwata, N.; Sata, N.; Tsurui, Takao; Yugami, H. *Jpn. J. Appl. Phys.* **2005**, *44*, 8613–8618.
- (18) Maekawa, H.; Fujimaki, Y.; Shen, H.; Kawamura, J.; Yamamura, T. *Solid State Ionics* **2006**, *117*, 2711–2714.
- (19) Maier, J. *Solid State Ionics* **1994**, *70*, 43–51.
- (20) Maier, J. *Solid State Ionics* **2002**, *154–155*, 291–301.
- (21) Maier, J. *Solid State Ionics* **2003**, *157*, 327–334.
- (22) Maier, J. *Nat. Mater.* **2005**, *4*, 805–815.

Belousov<sup>23</sup> have reviewed such enhancement of ionic conductivity in nanostructured conductors, “nanoionics,” from the viewpoints of defect chemistry and thermodynamics. Quantitative analyses of ionic conductivity at the heterointerfaces have also been demonstrated using the percolation and effective medium theory<sup>3,8,24</sup> and by molecular dynamics simulation.<sup>25</sup>

We previously reported the proton conductivity of nanometer-scale multilayers consisting of a polycation and a negatively charged proton conductor prepared via layer-by-layer (LbL) assembly.<sup>26,27</sup> The obtained polycation/proton conductor multilayer electrolytes are insoluble as well as thermally and chemically stable. LbL assembly has been widely used to fabricate various types of multilayered structure.<sup>28–34</sup> LbL assembly is mainly conducted through electrostatic interaction; oppositely charged materials, such as polyelectrolytes, are alternately deposited on a charged substrate. The dielectric and ion conduction properties of LbL films were first investigated by Durstock and Rubner.<sup>35</sup> DeLongchamp and Hammond reported the ionic conductivities of various types of polycation/polyanion film.<sup>36</sup> Recently, Tago et al. reported that a multilayered complex consisting of the polystyrene sulfonic acid and a polycation membrane prepared by LbL assembly is water-insoluble, thermostable, and shows high proton conductivities of  $\sim 1 \times 10^{-4}$  S/cm from 30 to 180 °C even under dry conditions.<sup>37</sup>

In this study, a high-proton conductor of Nafion and a polycation (poly(allylamine hydrochloride)) were alternately deposited on a glass substrate via LbL assembly, and the proton conduction mechanism through ultrathin Nafion layers was investigated. Nafion consists of strongly hydrophobic polytetrafluoroethylene chains and hydrophilic  $-\text{SO}_3^-$  groups. As shown in Figure 1, in a bulk Nafion membrane, a few-nanometer-diameter ionic clusters are formed.<sup>38</sup> On the other hand, in the multilayered LbL electrolyte, protons are considered to conduct through ultrathin Nafion layers, which are sandwiched between positively charged polycations.

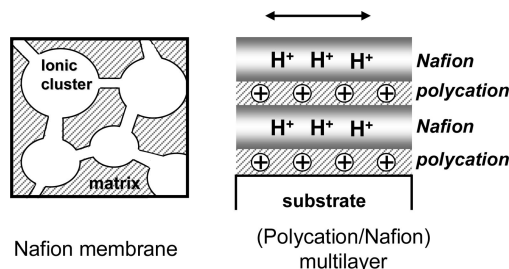


**Figure 1.** Schematic illustration of bulk Nafion membrane and (polycation/Nafion)<sub>n</sub> multilayer prepared via LbL assembly. For LbL multilayers, proton conductivity in the direction parallel to the substrate shown as an arrow was measured using a comb electrode.

Electric charge density and Debye shielding intensity, which are directly related to the thickness of a layer, are expected to significantly affect proton conductivity. In this paper, we report for the first time the deposition of thickness-controlled Nafion ultrathin layers and the proton mobilities of various multilayers. The conductivity and mobility of protons are elaborated on the basis of the analysis results of the electric charge density of polycation/Nafion multilayers.

## Experimental Procedure

**Deposition of the Ultrathin Nafion Layer.** Poly(diallyldimethylammonium chloride) (PDDA, weight-average molecular mass  $M = 100\,000$ – $200\,000$  g mol<sup>-1</sup>, Aldrich), poly(ethylenimine) (PEI,  $M = 500\,000$ – $1\,000\,000$ , Sci. Polym. Products), poly(allylamine hydrochloride) (PAH,  $M = 15\,000$ , Aldrich), poly(sodium 4-styrenesulfonate) (PSS,  $M = 70\,000$  g mol<sup>-1</sup>, Aldrich), and Nafion solution (5 wt % in a mixture of lower aliphatic alcohols and 15–20% water, Aldrich) were used as purchased. PDDA, PEI, and PAH are polycations, and PSS and Nafion are polyanions. The molecular structures of the polycations and polyanions used are shown in Figure 2a.

A quartz crystal microbalance (QCM, UEQ-400Easy, USI Co., Ltd.) was used for monitoring the adsorption of layers. A gold-evaporated QCM electrode (AT-cut) with a resonance frequency of 9 MHz was used. Before each QCM experiment, the QCM electrode was cleaned with a piranha solution (98% H<sub>2</sub>SO<sub>4</sub>:30% H<sub>2</sub>O<sub>2</sub> = 3:1, v/v), rinsed with pure water, and dried with nitrogen gas. After cleaning, the electrode was first immersed in a PEI solution for 10 min, followed by rinsing with pure water for 3 min and drying with nitrogen gas, and then weighed in an ambient atmosphere at room temperature. The PEI-coated electrode was further immersed in PSS and PDDA solutions alternately each for 10 min to prepare precursor layers of PEI/PSS/PDDA/PSS to increase the surface charge density. The polymer solutions containing 0.5 M NaCl were used: the concentrations of PEI, PDDA, and PSS were 1 mg/mL.

The primer-coated electrode was alternately immersed in a PAH solution and then in a Nafion solution for 10 min. After each adsorption step, the electrode was washed and dried with nitrogen gas and then weighed in an ambient atmosphere at room temperature. An ammonia–water solution was used to control the pH of the PAH solution (pH = 3.3, 4.7, 7.7, 8.8, and 10.0). A PAH solution (1 mg/mL) containing 0.5 M NaCl and a Nafion solution (1 mg/mL 90 vol MeOH/water mixture) were used for the LbL assembly.

For the proton conductivity and  $\zeta$ -potential measurements, a nonalkaline glass substrate (NH Techno Glass, NA35) was used. The PAH and Nafion multilayers were deposited on the glass substrate with an area of  $7.5 \times 4.0$  cm<sup>2</sup>, and then the Nafion-

- (23) Belousov, V. V. *J. Eur. Ceram. Soc.* **2007**, *27*, 3459–3467.
- (24) Matsumoto, H.; Furuya, Y.; Okada, S.; Tanji, T.; Ishihara, T. *Sci. Technol. Adv. Mater.* **2007**, *8*, 531–535.
- (25) Sayle, D. C.; Doig, J. A.; Parker, S. C.; Watson, G. W.; Sayle, T. T. *Phys. Chem. Chem. Phys.* **2005**, *7*, 16–18.
- (26) Daiko, Y.; Katagiri, K.; Shimoike, K.; Sakai, M.; Matsuda, A. *Solid State Ionics* **2007**, *178*, 621–625.
- (27) Daiko, Y.; Sakamoto, H.; Katagiri, K.; Muto, H.; Sakai, M.; Matsuda, A. *J. Electrochem. Soc.* **2008**, *155*, B479–B482.
- (28) Ariga, K.; Hill, P.; Ji, Q. *Phys. Chem. Chem. Phys.* **2007**, *9*, 2319–2340.
- (29) Decher, G.; Schlenoffeds, J. *Multilayer Thin Films. Sequential Assembly of Nanocomposite Materials*; Wiley-VCH GmbH: Weinheim, 2003.
- (30) Caruso, F.; Caruso, R. A.; Möhwal, H. *Science* **1998**, *282*, 1111–1114.
- (31) Caruso, F.; Schüler, C.; Kurth, D. G. *Chem. Mater.* **1999**, *11*, 3394–3399.
- (32) Alexandra, S. A.; Katagiri, K.; Caruso, F. *Soft Matter* **2006**, *2*, 18–23.
- (33) Sukhishvili, S. A.; Granick, S. *Macromolecules* **2002**, *35*, 301–310.
- (34) Stair, J. L.; Harris, J. J.; Bruening, M. L. *Chem. Mater.* **2001**, *13*, 2641–2648.
- (35) Durstock, F. M.; Rubner, F. M. *Langmuir* **2001**, *17*, 7865–7872.
- (36) DeLongchamp, D. M.; Hammond, P. T. *Chem. Mater.* **2003**, *15*, 1165–1173.
- (37) Tago, T.; Shibata, H.; Nishide, H. *Macromol. Symp.* **2006**, *235*, 19–24.
- (38) Mauritz, K. A.; Moore, R. B. *Chem. Rev.* **2004**, *104*, 4535–4586.

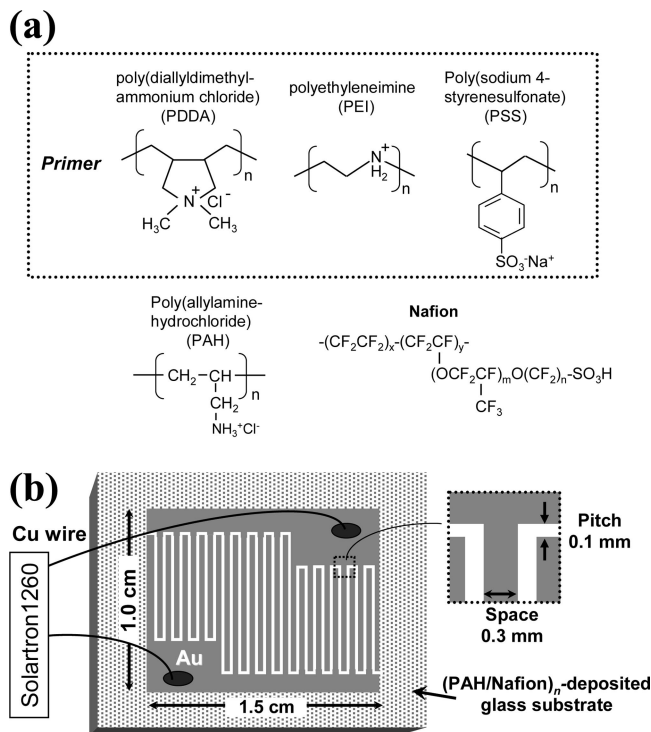


**Figure 2.** (a) Molecular structures of polycations and polyanions and (b) shape of evaporated Au comb electrode.

deposited glass substrate was cut into  $1.5 \times 2.0 \text{ cm}^2$  pieces for both conductivity and  $\zeta$ -potential measurements. Prior to the LbL deposition, glass substrates were soaked in a  $\text{H}_2\text{O}_2/\text{NH}_4\text{OH}$  aqueous mixture (30%  $\text{H}_2\text{O}_2$ :28%  $\text{NH}_4\text{OH}$ : $\text{H}_2\text{O}$  = 1:1:5 in volume ratio) at  $70^\circ\text{C}$  for 15 min, followed by rinsing with deionized water and finally drying with nitrogen gas. The resultant glass substrates were charged negatively in water owing to free  $-\text{OH}$  groups on the surface. Primer layers of PDDA/PSS/PDDA/PSS and then the  $(\text{PAH}/\text{Nafion})_n$  ( $n$ : the number of layers, in this study,  $n = 1-4$ ) multilayer were deposited on the glass substrates following the same procedures as those for the QCM electrodes.

The electric conductivity of the samples was determined from Cole–Cole plots obtained by an AC method using an impedance analyzer (Solartron 1260) with frequencies ranging from 1 to 100 kHz. The gold electrode shown in Figure 2b was evaporated on the multilayered film. The proton conductivity ( $\sigma$ ) of the  $(\text{PAH}/\text{Nafion})_n$  multilayer was calculated as

$$\sigma = f/(Rd) \quad (1)$$

where  $f$  is the constant related to the shape of the gold electrode,  $R$  is the resistance, and  $d$  is the total thickness of the deposited layers. Proton conductivity in the direction parallel to the substrate was measured using a comb electrode shown in Figure 2b.

The  $\zeta$ -potential of the films deposited on the glass substrates was measured using a  $\zeta$ -potential analyzer (Otsuka electronics, ELS-8000). Monitor particles (400 nm polystyrene) dispersed in 10 mM NaCl solution were used.

## Results and Discussion

**Deposition of the Ultrathin Nafion Layer.** A weak polycation of PAH was used to prepare ultrathin Nafion multilayers. The solution  $\text{p}K_a$  of PAH is about 9.0. The incremental film growth of the  $(\text{PAH}/\text{Nafion})_n$  multilayers ( $n$  is the number of layers) deposited using PAH solutions

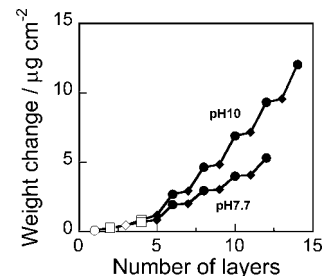


**Figure 3.** Changes in amounts of deposited layers calculated from QCM frequency decrease ( $-\Delta F$ ): PEI ( $\circ$ ), PSS ( $\square$ ), PDPA ( $\diamond$ ), PAH ( $\blacklozenge$ ), and Nafion ( $\bullet$ ).

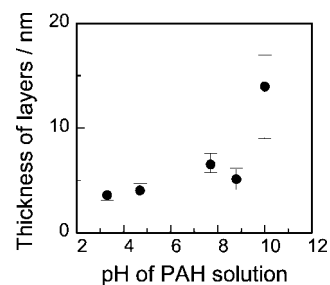


**Figure 4.** Relationship between thickness of Nafion layer in  $(\text{PAH}/\text{Nafion})$  multilayer and pH of the PAH solution.

(pH 7.7 and pH 10) is shown in Figure 3. The amounts of deposited PAH and Nafion layers increased almost linearly with increasing number of layers. This is due to the fact that multiple PAH/Nafion bilayers were deposited regularly and homogeneously. Note that the amount of the deposited Nafion layer increased significantly with increasing pH of the PAH solution from 7.7 to 10.

The thickness of each layer was calculated as

$$L = (0.0273 \times \Delta F) / \rho \quad (2)$$

where  $L$  is the thickness (nm) of a layer,  $\Delta F$  is the frequency shift of the results obtained using the QCM, and  $\rho$  is the layer density ( $1.64 \text{ g/cm}^3$  for Nafion<sup>39</sup> and  $1.2 \text{ g/cm}^3$  for PAH). Figure 4 shows the relationship between the pH of the PAH solution and the thickness of one Nafion layer. The thickness of the Nafion layer was changed from 3 to 15 nm by changing the pH of the PAH solution in the range from 3.3 to 10.0. Weak polyelectrolytes are ionic polymers with linear charge densities that are tunable by simple pH adjustment. The pH of a polyelectrolyte solution is crucial for controlling the charge density of an adsorbing polymer<sup>35,36</sup> and thus for controlling the thickness of a layer. The total thickness of the multilayers obtained using the QCM was used for the calculation of the proton conductivity.

**$\zeta$ -Potential of the  $(\text{PAH}/\text{Nafion})$  Multilayer.** Figure 5a–e shows the changes in  $\zeta$ -potential with the number of layers. Alternating  $\zeta$ -potentials were observed with the subsequent deposition of PAH and Nafion layers, suggesting the stepwise formation of multilayers on the nonalkaline glass substrate. However, the  $\zeta$ -potentials of both PAH and Nafion layers changed significantly when the pH of the PAH solution was varied. For example, when the PAH solution of  $\text{pH} = 7.7$  was used, large positive  $\zeta$ -potentials for PAH layers and small negative  $\zeta$ -potentials for Nafion layers were observed

(39) Saito, M.; Arimura, K.; Hayamizu, K.; Okada, T. *J. Phys. Chem. B* **2004**, *108*, 16064–16070.



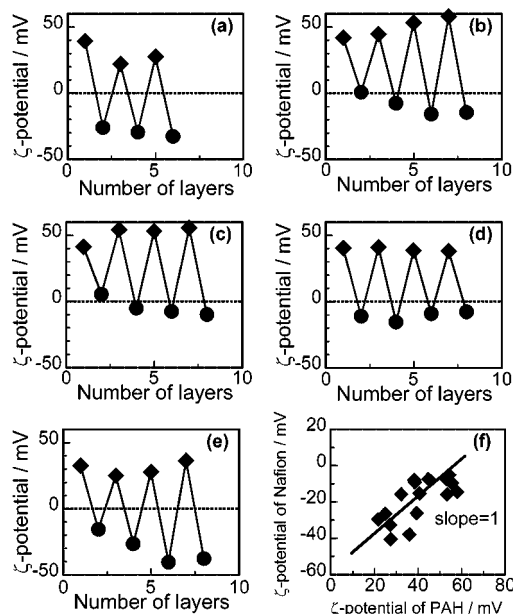


**Figure 5.** Changes in  $\zeta$ -potentials of PAH and Nafion layers with the number of layers. Various PAH solutions with different pH values were used for the deposition of (PAH/Nafion) $_n$  multilayers: (a) pH 3.3, (b) pH 4.7, (c) pH 7.7, (d) pH 8.8, and (e) pH 10.0. (f) Relationship between  $\zeta$ -potential of PAH and the following Nafion layer.

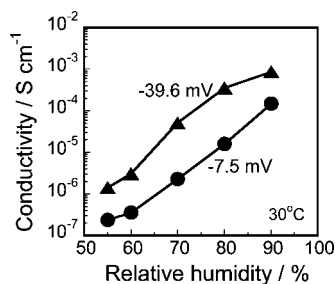
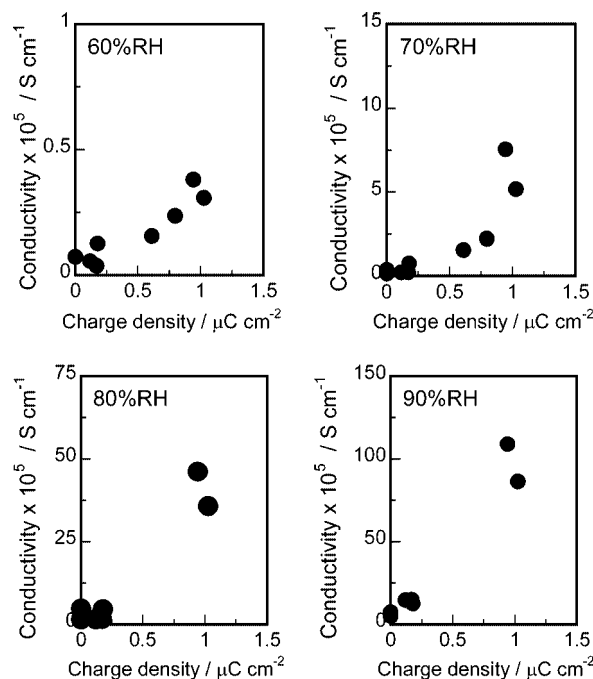


**Figure 6.** Relative humidity dependence of proton conductivity at 30 °C for (PAH/Nafion) $_4$  multilayers with  $\zeta$ -potentials of the outmost Nafion layer of  $-7.5$  and  $-39.6$  mV.

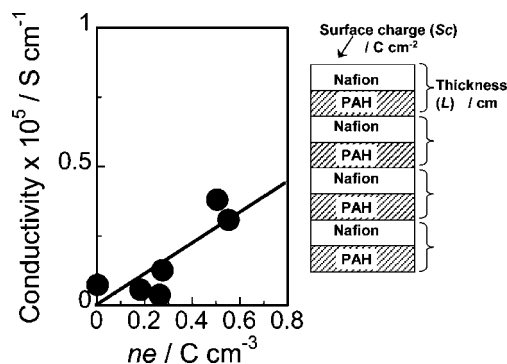
(Figure 5c). On the other hand, when the PAH solution of pH = 10 was used, relatively small positive  $\zeta$ -potentials for PAH layers and large negative  $\zeta$ -potentials for Nafion layers were observed (Figure 5e).

Figure 5f shows the relationship between the  $\zeta$ -potential of PAH and the following Nafion layers. When the pH of the PAH solution was increased, the charge density of PAH decreased as its ammonium groups became deprotonated. A linear relationship with slope = 1 was observed, suggesting that the surface charge density of Nafion, which is related to the number of free  $-\text{SO}_3^-$  groups, is dominated by the PAH charge density.

**Electric Charge Density and Proton Conductivity.** The proton conductivities of all the (PAH/Nafion) $_n$  ( $n = 1-4$ ) multilayers were measured at 30 °C. Results for the two types of multilayer with different  $\zeta$ -potentials in the outmost Nafion layer ( $-39.6$  and  $-7.5$  mV) are shown in Figure 6. The proton conductivities of both multilayers markedly increased with increasing relative humidity from 55 to 90%. The protons that dissociated from the free  $-\text{SO}_3^-$  groups in the Nafion layers are considered to hop through absorbed water



**Figure 7.** Relationship between surface charge densities calculated using eq 4 and proton conductivities at 30 °C and relative humidity (RH) of 60–90%.



**Figure 8.** Relationship between charge densities per unit volume ( $ne$ ) and proton conductivities at 30 °C and 60% RH.

molecules. Note that the multilayer with a large negative  $\zeta$ -potential showed higher proton conductivity.

The surface charge density is represented by the Poisson–Boltzmann equation

$$\frac{d^2\psi}{dx^2} = \frac{zen}{\epsilon_r\epsilon_0} \left[ \exp\left(\frac{ze\psi(x)}{kT}\right) - \exp\left(-\frac{ze\psi(x)}{kT}\right) \right] \quad (3)$$

From the differential equation (eq 3), the surface charge ( $Sc$ , C/cm $^2$ ) is given by

$$Sc = (2000N_A C \epsilon_r \epsilon_0 kT)^{1/2} \left[ \exp\left(\frac{ze\psi_0}{2kT}\right) - \exp\left(-\frac{ze\psi_0}{2kT}\right) \right] \quad (4)$$

where  $\psi_0$  is the surface potential ( $x = 0$ ; in this study, the measured  $\zeta$ -potential was used),  $k$  is the Boltzmann constant,  $T$  is the absolute temperature,  $e$  is the elementary electric charge,  $N_A$  is Avogadro's number,  $z$  and  $C$  are the valence and concentration of the solution ( $z$  is 1 and  $C$  is 10 mM), and  $\epsilon_r$  and  $\epsilon_0$  are the dielectric constants of the solution and vacuum ( $\epsilon_r$  is 78.5 and  $\epsilon_0$  is  $8.85 \times 10^{-12}$  F/m), respectively.

**Table 1. Proton Mobilities at 30 °C Obtained from the Slope in Figure 8 and Correlation Coefficients for the (PAH/Nafion)<sub>n</sub> Multilayer and Nafion 117 Membrane**

sample	relative humidity, %	$\mu \times 10^4$ , cm <sup>2</sup> V <sup>-1</sup> s <sup>-1</sup>	correlation coefficient
(PAH/Nafion) <sub>n</sub> multilayer	60	0.056	0.847
	70	0.94	0.852
	80	6.1	0.836
	90	15.2	0.876
Nafion 117		2.0	

The surface charge density was calculated from eq 4, and the proton conductivities of the (PAH/Nafion)<sub>n</sub> multilayers are plotted in Figure 7 as a function of the absolute value of the obtained charge density. Note that the proton conductivities increased almost linearly with increasing surface charge density of the outermost Nafion layer. The *Sc* of the outermost Nafion layer was observed to be related to the concentration of surface SO<sub>3</sub><sup>-</sup> groups.

As shown by the results obtained using the QCM, each PAH and Nafion layer was deposited regularly and homogeneously. The electric charge per unit volume (C/cm<sup>3</sup>), which corresponds to the *ne* in the following equation (eq 5), was thus estimated from the surface charge density (*Sc*) (C/cm<sup>2</sup>) shown in Figure 7 and the thickness of the PAH/Nafion bilayer (*L*) (cm).

$$\sigma = ne\mu \quad (5)$$

$$ne = Sc/L \quad (6)$$

Note that the obtained *ne* values were ~1 C/cm<sup>3</sup>, which are much lower than that of bulk Nafion (~160 C/cm<sup>3</sup>). The *ne* value is correlated with the number of mobile protons, and such small *ne* values for LbL films can be attributed to the formation of the -SO<sub>3</sub><sup>-</sup>...NH<sub>3</sub><sup>+</sup> ionic complex. Similar results have also been reported; for example, Farhat and Schlenoff reported that the number of mobile ions is limited because of the large extent of polyion pairing and rejection of residual small ions from the LbL film, which is especially notable in strong polyion systems such as PDDA/PSS.<sup>40</sup> DeLongchamp and Hammond discussed the relationship between the cross-link density and proton conductivity of LbL multilayers by using three different types of LbL films.<sup>36</sup> On the other hand, recent <sup>1</sup>H NMR analysis revealed a proton-proton interaction between polycation and polyanion in LbL films.<sup>41</sup>

Figure 8 shows the relationship between the calculated *ne* values and the proton conductivity of the (PAH/Nafion)<sub>n</sub> multilayer. The slope in Figure 8 directly corresponds to the proton mobility, and the obtained proton mobilities and correlation coefficients at 60–90% RH are summarized in Table 1. Note that the (PAH/Nafion)<sub>n</sub> multilayers showed an approximately 7-fold higher proton mobility (15.2 cm<sup>2</sup>/V s) than a bulk Nafion 117 membrane (2 × 10<sup>-4</sup> cm<sup>2</sup>/V s).<sup>42</sup> Although the number of free -SO<sub>3</sub><sup>-</sup> groups was

decreased by the formation of the ionic complex, the proton mobility of the LbL multilayer was increased markedly. These results suggest that further improvement of proton conductivity can be achieved by utilizing a proton conductor with a higher -SO<sub>3</sub><sup>-</sup> concentration than Nafion. In the bulk Nafion membrane, protons conduct through ionic clusters, which are connected to each other by very narrow (~1 nm) paths.<sup>38</sup> It was reported that the ionic channel structure of commercial bulk Nafion membranes is not expressed in LbL films.<sup>36</sup> One possible mechanism of the increase in proton mobility of LbL film is that the size of the conductive path of the (PAH/Nafion)<sub>n</sub> multilayers is larger than that of bulk Nafion.

The orientation of sulfo groups as well as the distribution of protons in Nafion layers should be affected by the Debye shielding intensity of the polycation layers, and the electrostatic repulse forces between protons in Nafion and the polycation of PAH layers should also considerably affect the mobility of protons. The results obtained here strongly suggest that the multilayered ultrathin electrolytes prepared via LbL assembly are one of the candidates for a new type of proton conductor. On the basis of the viewpoints of *Nanoionics*, investigations including the suitable design of multilayers and the detailed simulation of the charge distribution of the ultrathin multilayers are in progress to understand the mechanism of proton conduction and to achieve higher proton conductivities.

## Conclusion

The proton conductivity and mobility of ultrathin (PAH/Nafion)<sub>n</sub> multilayers prepared via LbL assembly have been investigated. A good linear relationship is observed between the ζ-potential of the outmost Nafion layer and the proton conductivity. The analysis of the electric charge density suggests that the proton mobility of the PAH/Nafion multilayers is approximately sevenfold higher than that of a bulk Nafion membrane. LbL assembly offers an easy and inexpensive solution process and allows various materials to be incorporated within the film structures. In addition, the obtained multilayer electrolytes are insoluble as well as thermally and chemically stable. The nanostructured multilayers prepared via LbL assembly are a promising candidate for a new type of proton conductor, in which protons conduct through an ultrathin space surrounded by positive charges.

**Acknowledgment.** This work has been supported by the New Energy and Industrial Technology Development Organization (NEDO) project "Development of Technology for Next-Generation Fuel Cells" and by the Ministry of Education, Culture, Sports, Science and Technology (MEXT) of Japan (Grant-in-Aid for Young Scientists (Startup), No. 18850009, 2006, and Exploratory Research, No. 19656169, 2007).

CM8007705

(40) Farhat, T. R.; Schlenoff, J. B. *Langmuir* **2001**, *17*, 1184–1192.

(41) Rodriguez, L. N. J.; De Paul, S. M.; Barrett, C. J.; Reven, L.; Spiess, H. W. *Adv. Mater.* **2000**, *12*, 1934–1938.

(42) Daiko, Y.; Katagiri, K.; Ogura, K.; Sakai, M.; Matsuda, A. *Solid State Ionics* **2007**, *178*, 601–605.